Electronic Structure of Carbon Trioxide and Vibronic Interactions Involving Jahn−Teller States

Timothy Kowalczyk and Anna I. Krylov*

Department of Chemistry, University of Southern California, Los Angeles, California 90089-0482

Received: May 11, 2007; In Final Form: June 14, 2007

The electronic structure of CO_3 is characterized by equation-of-motion and coupled-cluster methods. C_{2v} and D_{3h} isomers are considered. Vertical excitation energies, transition dipoles, and the molecular orbital character of the excited states are presented for singlet and triplet manifolds. Ground-state equilibrium structures and frequencies are strongly affected by vibronic interactions with low-lying excited states. At D_{3h} geometries, the vibronic interactions are enhanced by the Jahn−Teller character of the excited states. The curvature of the potential energy surface and the existence of the D_{3h} minimum are very sensitive to the correlation treatment and the basis set. The correlation effects are stronger at D_{3h}, in agreement with a smaller HOMO−LUMO gap.

1. Introduction

Complex reactions of carbon mono- and dioxide with atomic oxygen in planetary (for example, Martian) and terrestrial atmospheres are thought to involve carbon trioxide, which has been characterized both experimentally and theoretically.[1−10] From the first studies, two isomers, D_{3h} and C_{2v}, were considered. The vibrational spectra[1,2,8] are consistent with C_{2v} structure. However, the calculations[5,8,9] predict that the two isomers are very close in energy; for example, Kaiser and co-workers have found two minima to be within 0.1 kcal/mol from each other and separated by a modest barrier of 4 kcal/mol using multiconfigurational self-consistent field (MCSCF) optimized geometries and multireference configuration interaction energies. Recently, Kaiser and co-workers reported the first spectroscopic identification of the D_{3h} isomer in CO_2 ice.[10]

Except for the lowest triplet state,[5,6,8] electronically excited states of carbon trioxide attracted much less attention, despite their role in the C_{2v} vs D_{3h} competition.[4] Random phase approximation (RPA) excitation energies for several lowest singlets of the C_{2v} isomer were reported by Canuto and Diercksen.[11] Some stationary points of the lowest singlet potential energy surface (PES) were calculated by Mebel and co-workers.[8] Several triplet states were characterized by Averyanov et al.[6]

In this work, we characterize low-lying electronic states of CO_3 at D_{3h} and C_{2v} configurations. At D_{3h}, the lowest excited states form degenerate pairs. In accordance with the Jahn−Teller (JT) theorem, the energies of these states depend linearly on C_{2v} displacements that lift the degeneracy. This JT behavior of the excited states enhances vibronic interactions with the ground state, which strongly affects the shape of the ground-state PES, especially its curvature along $D_{3h} \rightarrow C_{2v}$ displacements. We present the optimized geometries, relative energies, and harmonic frequencies for the D_{3h} and C_{2v} structures and analyze the results in terms of vibronic interactions and orbital (near-) instabilities.

The structure of the paper is as follows. The next section discusses vibronic interactions involving JT states. Section 3 summarizes computational details. Section 4 presents molecular orbital framework, excited states, and the shape of the PES along $D_{3h} \rightarrow C_{2v}$ structures. Our concluding remarks are given in section 4.2.

2. Vibronic Interactions Involving Jahn−Teller States

The competition between higher and lower symmetry structures often referred to as symmetry breaking is quite common in electronic structure.[12] Several recent studies[13−17] discussed different aspects of symmetry breaking in ab initio calculations distinguishing between (i) purely artefactual spatial and spin symmetry breaking of approximate wave functions, that is, the Löwdin dilemma,[18] and (ii) real interactions between closely lying electronic states that result in lower-symmetry structures, significant changes in vibrational frequencies (see Figure 1 from ref 15), and even singularities (first-order poles) in force constants (for example, Figure 3 from ref 14).

Formally, the effect of the interactions between electronic states on the shape of potential energy surface can be described[14] by the Herzberg−Teller expansion of the potential energy of electronic state i:

$$V_i = V_0 + \sum_\alpha \left\langle \Psi_i \left| \frac{\partial H}{\partial Q_\alpha} \right| \Psi_i \right\rangle Q_\alpha + \frac{1}{2} \sum_\alpha \left\langle \Psi_i \left| \frac{\partial^2 H}{\partial^2 Q_\alpha} \right| \Psi_i \right\rangle Q_\alpha{}^2 - \sum_\alpha \sum_{j \neq i} \frac{\left(\left\langle \Psi_i \left| \frac{\partial H}{\partial Q_\alpha} \right| \Psi_j \right\rangle \right)^2}{E_j - E_i} Q_\alpha{}^2 \quad (1)$$

where Q_α denotes normal vibrational modes and wave functions Ψ_k and energies E_k are adiabatic wave functions and electronic energies at $Q_\alpha = 0$. The last term, which is quadratic in nuclear displacement (hence *second*-order Jahn−Teller) describes vibronic effects. For the ground state, that is, when $E_j > E_i$, it causes softening of the force constant along Q_α, which may ultimately result in a lower-symmetry structure, for example, Figure 1 from ref 15. The above-mentioned poles in force constants originate in the energy denominator. As discussed by Crawford and co-workers,[19] the couplings described by eq 1

10.1021/jp073627d CCC: $37.00
Published on Web 07/28/2007

can be related to RHF orbital instabilities and near-instabilities, which often result in spurious frequencies. The effect of vibronic interactions on the curvature of the ground-state PES of CO_3 was first discussed by Guchte et al.[4]

Although numerous examples of systems with strong vibronic interactions have been reported and analyzed in terms of eq 1, carbon trioxide presents three rather interesting features. First, there are several low-lying excited states (see section 4.1) that can interact with the ground state. Second, more than one vibrational mode Q_α are vibronically active: those are the in-plane CO stretching and bending motions. As discussed below, the curvature of the PES along these two modes is strongly affected by the vibronic interactions. Third, the JT behavior of the perturbing states reduces the energy denominator upon lower-symmetry distortions, which enhances the vibronic interactions.

It should be noted that CO_3 is isoelectronic with NO_3^- and shares a number of similarities with the infamous NO_3 radical.[16] The PES of the latter is strongly affected by vibronic interactions with a low-lying (JT) state and its harmonic vibrational levels calculated using Born−Oppenheimer PES are simply qualitatively incorrect, as demonstrated in the recent treatise by Stanton.[16]

The effect of the JT character of the perturbing state can be demonstrated by a model Hamiltonian of two states $U_1(Q)$ and $U_2(Q)$ coupled by the vibronic interaction term $V(Q)$:

$$H = \begin{pmatrix} U_1 & V \\ V & U_2 \end{pmatrix} \tag{2}$$

which gives rise to the two eigenstates $E_{1,2}(Q)$:

$$E_{1,2} = \frac{U_1 + U_2}{2} \mp \sqrt{\left(\frac{U_1 - U_2}{2}\right)^2 + V^2} \tag{3}$$

Following eq 1, we choose the following form for the coupling term:

$$V(Q) = K_\nu Q^2 \tag{4}$$

At the symmetric configuration $Q = 0$, V is zero and $E_i \equiv U_i$. If the energy gap between the states, $\Delta U = U_2 - U_1$, is small and U_1 and U_2 are parallel along Q, that is, $U_1(Q) \approx U_2(Q) = U(Q)$, then $E_{1,2}(Q) \approx U(Q) \mp K_\nu Q^2$. Thus, the quadratic force constant of the lower state is reduced by the value of K_ν. If, however, the energy of the second state $U_2(Q)$ contains a linear JT term, then $|U_1(Q) - U_2(Q)| = \Delta U + K_u Q$ and

$$E_1 = \frac{U_1 + U_2}{2} - \sqrt{\frac{\Delta U^2}{4} + \Delta U K_u Q + \left(\frac{K_u^2}{4} Q^2 + K_\nu^2 Q^4\right)} \approx U(Q) - \sqrt{\left(\frac{K_u^2}{4} Q^2 + K_\nu^2 Q^4\right)} \tag{5}$$

Thus, the magnitude of the coupling term and, consequently, the contribution to the quadratic force constant increases proportionally to K_u^2. Therefore, for the same $\Delta U(Q{=}0)$ and K_ν, the change in the shape of the lower surface, $E_1(Q)$, will be more pronounced when the upper state $U_2(Q)$ has linear terms.

3. Computational Details

Equilibrium geometries and vibrational frequencies were calculated by Möller−Plesset perturbation theory (MP2), as well as coupled-cluster methods with single and double excitations (CCSD), and with perturbative account of triples, CCSD(T), with 6-31G* and cc-pVTZ basis sets. Additional single-point calculations were performed using cc-pVQZ and aug-cc-pVTZ bases, as well as by the coupled-cluster model including full triples, CCSDT. All single-point energy calculations were carried out with frozen 1s orbitals.

Excitation energies were calculated by the equation-of-motion method for excitation energies with single and double substitutions, EOM-EE-CCSD,[20−22] and by EOM-EE(2,3),[23,24] which includes triple excitations in the EOM part. EOM-CCSD calculations employed 6-31G* and cc-pVTZ bases, whereas EOM-EE(2,3) calculations used 6-31G*. EOM-EE(2,3)/cc-pVTZ values are extrapolated using the energy additivity scheme:

$$E_{\mathrm{EOM(2,3)}}^{\mathrm{cc-pVTZ}} = E_{\mathrm{EOM-CCSD}}^{\mathrm{cc-pVTZ}} + (E_{\mathrm{EOM(2,3)}} - E_{\mathrm{EOM-CCSD}})^{\mathrm{6-31G^*}} \tag{6}$$

For well-behaved molecules, CCSD(T)/cc-pVTZ yields reliable molecular structures and frequencies;[25] however, in the case of strong nondynamical correlation and/or Hartree−Fock instabilities, its accuracy may deteriorate. The EOM-EE-CCSD errors for singly excited states are 0.1−0.3 eV for closed-shell molecules; however, if the reference state acquires significant multiconfigurational character, the weights of doubly excited configurations in the excited states increases, which eventually will result in the breakdown of EOM treatment. The inclusion of full triples improves the results for the ground and excited states, and the magnitude of the effect serves as a gauge of the quality of CCSD/EOM-CCSD results. With full triples, the errors in ground-state energy differences are expected to be less than 1 kcal/mol, and in the excitation energies, below 0.01 eV for singly excited states and 0.1 eV for the problematic doubly excited states.[23,24]

EOM-EE-CCSD and EOM-EE(2,3) results were obtained with the Q-Chem[26] ab initio package. CCSD(T) and CCSDT calculations were performed with the Aces II[27] electronic structure program.

4. Results and Discussion

4.1. Molecular Orbital Framework and Excited States. Twenty-two valence electrons of CO_3 occupy seven molecular orbitals (MOs) derived from four 2s and three in-plane p-orbitals that form a σ-like framework, as well as four π-like MOs. Relevant occupied and virtual MOs are shown in Figure 1. At D_{3h}, the highest occupied MOs are two pairs of doubly degenerate lone-pair orbitals. The HOMO is in-plane lp_σ, and the HOMO−1 is out-of-plane lp_π. At C_{2v}, the degeneracies are lifted, and some lone-pair orbitals acquire bonding OO and/or CO characters, as reflected by notations in Figure 1.

The two lowest unoccupied MOs are lp_σ^* and π^*-like at both geometries. The HOMO−LUMO gap is smaller at D_{3h}, resulting in stronger correlation effects and low-lying excited states.

Vertical excitation energies and transition dipole moments for both structures are presented in Tables 1 and 2 and in Figure 2. The character and ordering of the excited states is quite unusual.

At D_{3h}, the lowest excited states are derived from the $lp_\pi \rightarrow lp_\sigma^*$ and $lp_\sigma \rightarrow lp_\sigma^*$ excitations. They form two singlet and two triplet JT pairs. Triplets are barely above 1 eV, and the singlets are at about 1.3 and 3.3 eV. The vibronic interactions of these states with the ground state are quite strong and have a dramatic effect on the PES curvature along two different C_{2v} displacements, as discussed in the next section. At C_{2v}, the two lowest excited states in the singlet and triplet manifolds are also derived

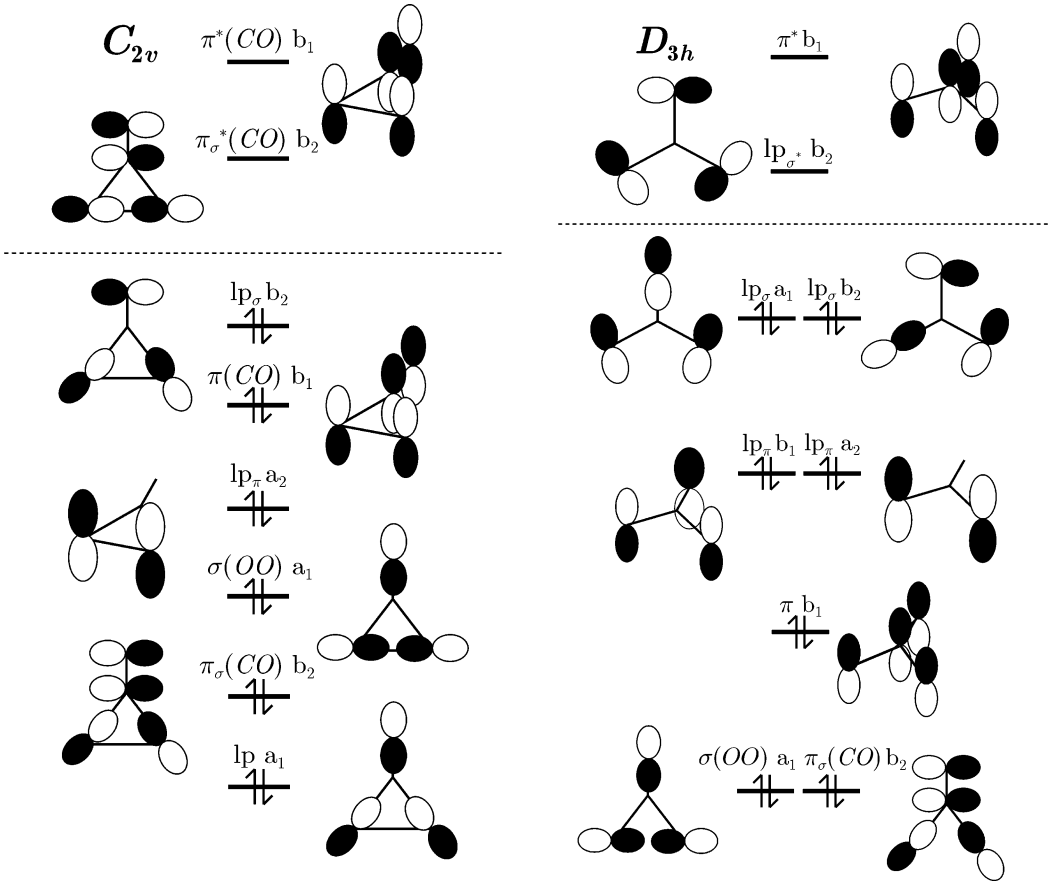

Figure 1. Relevant molecular orbitals and the ground-state electronic configuration of CO_3 at C_{2v} (left) and D_{3h} (right) geometries.

TABLE 1: Excitation (eV) Energies and Transition Dipole Moments (au, in Parentheses) of the C_{2v} Isomer Calculated by the EOM-EE-CCSD and EOM-EE(2,3) Methods

state	EOM-CCSD/6-31G*	EOM-CCSD/cc-pVTZ	EOM(2,3)/6-31G*	EOM(2,3)/cc-pVTZ, extrp-d
2^1A_1 $lp_\sigma \rightarrow \pi_\sigma^*(CO)$	4.81 (0.0000)	4.77 (0.0000)	4.68	4.65
3^1A_1 $\pi_\sigma(CO) \rightarrow \pi_\sigma^*(CO)$	9.31 (0.0000)	9.22 (0.0000)	9.03	8.94
1^1A_2 $\pi(CO) \rightarrow \pi_\sigma^*(CO)$	5.38 (0)	5.40 (0)	5.25	5.47
2^1A_2 $lp_\sigma \rightarrow \pi^*(CO)$	7.78 (0)	7.77 (0)	8.20	8.19
1^1B_2 $lp_\pi \rightarrow \pi^*(CO)$	8.35 (0.0290)	8.32 (0.0442)	8.37	8.34
2^1B_2 $\sigma \rightarrow \pi_\sigma^*(CO)$	9.59 (0.0149)	9.56 (0.0149)	9.40	9.35
1^1B_1 $lp_\pi \rightarrow \pi_\sigma^*(CO)$	3.30 (0.0021)	3.26 (0.0039)	3.59	3.55
1^3A_1 $lp_\sigma \rightarrow \pi_\sigma^*(CO)$	4.18	4.16	4.17	4.15
2^3A_1 $\pi_\sigma(CO) \rightarrow \pi_\sigma^*(CO)$	7.92	7.93	8.45	8.45
1^3A_2 $\pi(CO) \rightarrow \pi_\sigma^*(CO)$	5.05	5.05	5.07	5.07
2^3A_2 $lp_\sigma \rightarrow \pi^*(CO)$	7.48	7.48	7.96	7.96
1^3B_2 $lp_\pi \rightarrow \pi^*(CO)$	4.75	4.67	5.17	5.09
2^3B_2 $\sigma \rightarrow \pi_\sigma^*(CO)$	8.45	8.48	8.51	8.54
1^3B_1 $lp_\pi \rightarrow \pi_\sigma^*(CO)$	2.11	2.15	2.44	2.48

from $lp_\pi \rightarrow \pi_\sigma^*(CO)$ and $lp_\sigma \rightarrow \pi_\sigma^*(CO)$; however, the energy gap between the ground and excited states is much larger, that is, about 2.4 and 3.6 eV for the triplet and singlet manifolds, respectively.

At C_{2v}, the low-lying states are dominated by single excitations, and inclusion of triples has a moderate effect—the largest correction of 0.3 eV is for the lowest singlet and triplet states. Basis set dependence is also modest.

The first interesting feature is a relatively small energy gap, about 1 eV and less, between singlet and triplet states of the same character. The smallest gap (0.4 eV) is in between $\pi(CO) \rightarrow \pi_\sigma^*$ (CO), due to the different nodal structure of the initial and target MOs, which reduces the Coulomb repulsion in the singlet.

The second interesting feature is that the HOMO → LUMO excited state is not the lowest excited state. The lowest excited states in the triplet and the singlet manifolds are at 2.5 and 3.5 eV, respectively, and are derived from the HOMO−2, nonbonding lp_π, to the LUMO, $\pi_\sigma^*(CO)$. The oscillator strength for the singlet state is very small, due to disjoint character of the initial and target MOs, which is also responsible for the unusual state ordering. The HOMO → LUMO excited states, $^3A_1$ and $^1A_1$ are at 4.15 and 4.65 eV, respectively, closely followed by the HOMO−1 → HOMO pair around 5 eV. Among the low-lying excited states from Table 1 the largest transition dipole is obtained for the $lp_\pi \rightarrow \pi^*(CO)$ state, which is located at 8.34 eV.

At D_{3h}, the gap between the ground and excited states is smaller, which is consistent with the small HOMO−LUMO gap.

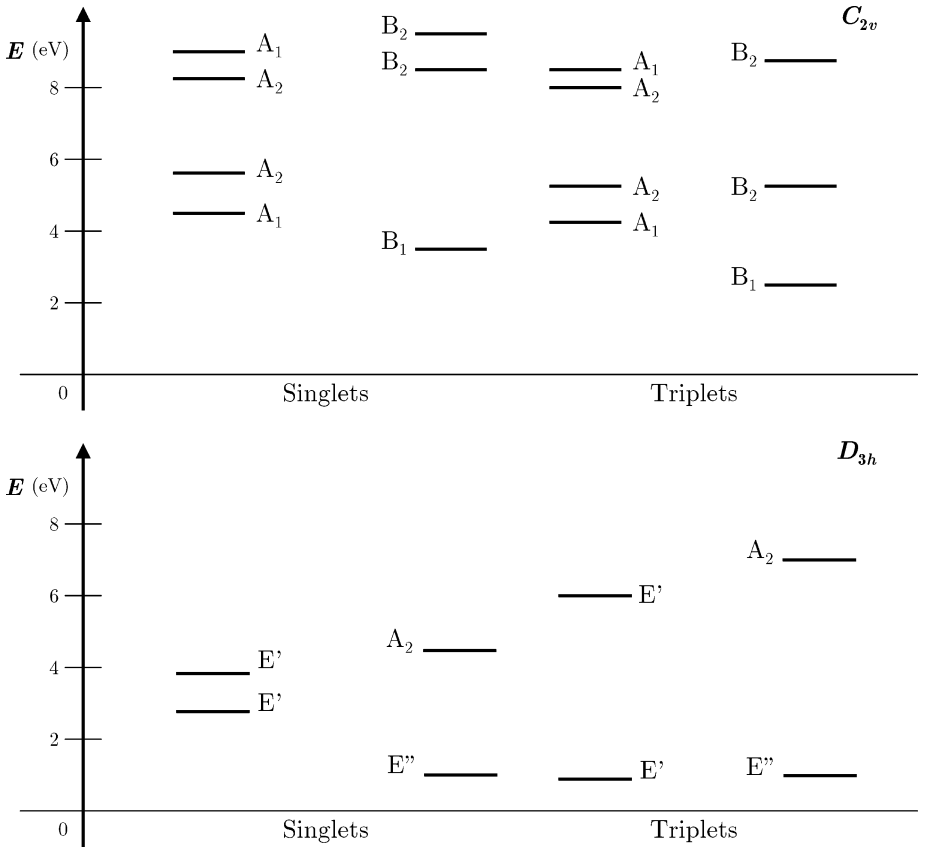

Figure 2. Electronically excited states of the C_{2v} (upper panel) and D_{3h} (lower panel) isomers of CO_3.

Consequently, some of the states acquire doubly excited character, and the inclusion of triples has more pronounced effect.

All low-lying states at D_{3h} are derived from the excitations to LUMO, lp_σ^*. The energy separations between the singlet and triplet states of the same character are, again, small, and the six lowest states in each multiplicity form three JT pairs. The two lowest JT pairs are derived from in-plane (σ-like) and out-of-plane (π-like) lone pairs. The corresponding $^3E'$ and $^3E''$ states are almost degenerate and located at 1.1−1.2 eV. The gap between the corresponding singlets is larger—$^1E''$ and $^1E'$ states are at 1.33 and 3.23 eV, respectively. Note that the relative ordering of E′ and E″ pairs is different for the singlet and triplet manifolds. In the triplet manifold, the lowest pair, E′, is derived from HOMO−LUMO excitations, whereas in the singlet manifold the E″ pair is lower, probably because of the reduced Coulomb repulsion due to the different nodal structure of the lp_π and lp_σ^* orbitals.

Note that the lowest singlet states are of E″ symmetry and therefore cannot affect e′ modes through vibronic couplings—it is the two next pairs of singlet E′ states that are responsible for the couplings.

4.2. Shape of the Ground-State PES along $D_{3h} \rightarrow C_{2v}$ Distortions. Optimized C_{2v} and D_{3h} geometries are shown in Figure 3. Changes in bond lengths calculated by different methods follow systematic trends.[25] For example, MCSCF generally overestimates bond lengths, due to the absence of dynamical correlation. MP2 is in good agreement with very accurate CCSD(T) in cases when nondynamical correlation is small (that is, at C_{2v} geometry); however, it overestimates antibonding character when the HOMO−LUMO gap is small, as happens at D_{3h}. Overall, larger differences between the methods at D_{3h}, that is, up to 0.015 Å between MP2 or CCSD

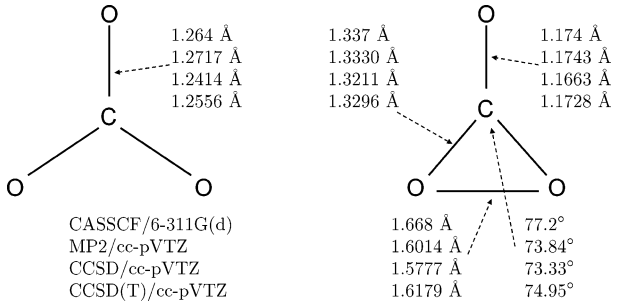

Figure 3. Ground-state optimized geometries of two CO_3 isomers calculated by the MP2, CCSD, and CCSD(T) methods with the cc-pVTZ basis. The CASSCF/6-311G(d) geometry from ref 8 is also given.

and CCSD(T), as opposed to 0.001−0.008 Å at C_{2v}, are consistent with a smaller HOMO−LUMO gap and the presence of low-lying excited states at D_{3h}. The MCSCF bond lengths are within 0.001−0.008 Å from the CCSD(T) values for both structures, except for the OO bond at C_{2v}, which is overestimated by 0.05 Å.

As far as structural differences between the isomers are concerned, the CO bond length disproportionates almost evenly upon the change from D_{3h} to C_{2v}: from 1.256 Å to 1.173 Å and 1.330 Å, that is, by −0.083 and +0.074 Å, respectively. These values could be compared with the bond length in CO (triple bond) and CO_2 (double bond) calculated at the same level of theory, which are 1.133 and 1.163 Å. Thus, the short r_{CO} in the C_{2v} isomer is very close to the double CO bond length.

The vibrational frequencies are given in Table 3. Although frequencies of the C_{2v} isomer exhibit moderate dependence (several percents) on the basis set or correlation treatment, the D_{3h} structure features dramatic variations for the two JT active modes, CO stretch and bend. The former drops from 3300 cm^{-1} (MP2 value) to about 1400−1100 cm^{-1} at the CCSD or

TABLE 2: Excitation (eV) Energies and Transition Dipole Moments (au, in Parentheses) of the D_{3h} Structure Calculated by the EOM-EE-CCSD and EOM-EE(2,3) Methods

state	EOM-CCSD/6-31G*	EOM-CCSD/cc-pVTZ	EOM(2,3)/6-31G*	EOM(2,3)/cc-pVTZ, extrp-d
$1^1E'$ ($2^1A_1/1^1B_2$) $lp_\sigma \rightarrow lp_{\sigma^*}$	3.60 (0.5220)	3.57 (0.5343)	3.27	3.23
$2^1E'$ ($3^1A_1/2^1B_2$) σ_{OO}, π_σ(CO) $\rightarrow lp\sigma^*$	5.68 (0.2695)	5.80 (0.3229)	3.81	3.93
$1^1E''$ ($1^1A_2/1^1B_1$) $lp_\pi \rightarrow lp_{\sigma^*}$	1.32 (0.0000)	1.32 (0.0000)	1.34	1.33
2^1A_2 $\pi \rightarrow lp_{\sigma^*}$	5.57 (0.0000)	5.56 (0.0000)	4.37	4.36
$1^3E'$ ($1^3A_1/1^3B_2$) $lp_\sigma \rightarrow lp_{\sigma^*}$	0.43	0.33	1.20	1.10
$2^3E'$ ($2^3A_1/2^3B_2$) σ_{OO}, π_σ(CO) $\rightarrow lp_{\sigma^*}$	5.90	5.76	6.15	6.02
$1^3E''$ ($1^3A_2/1^3B_1$) $lp_\pi \rightarrow lp_{\sigma^*}$	0.91	0.88	1.20	1.18
2^3A_2 $\pi \rightarrow lp_{\sigma^*}$	5.71	5.65	7.12	7.06

TABLE 3: Harmonic Vibrational Frequencies, cm^{-1}, and Infrared Intensities (in Parentheses) of the Two CO_3 Structures

C_{2v} Isomer						
mode/symmetry	MP2/6-31G*	MP2/cc-pVTZ	CCSD/6-31G*	CCSD cc-pVTZ	CCSD(T)/6-31G*	CCSD(T)/cc-pVTZ
bend/b_1	553	562	546	569	555	575 (7.8)
bend/a_1	658	667	693	675	620	606 (10.3)
OPLA/b_2	623	686	598	665	625	683 (30.2)
CO stretch/b_1	1037	1088	1074	1024	1057	1007 (61.4)
OCO stretch/a_1	1138	1106	1184	1140	1141	1099 (15.6)
CO stretch/a_1	2170	2085	2243	2138	2181	2078 (524.8)
D_{3h} Structure						
mode/symmetry	MP2/6-31G*	MP2/cc-pVTZ	CCSD/6-31G*	CCSD cc-pVTZ	CCSD(T)/6-31G*	CCSD(T)/cc-pVTZ
bend/e′	676	672	179	−292	−300	−402
OPLA/a_2''	688	746	730	756	707	776 (24.2)
CO stretch/e′	3341	3501	1388	1263	1208	1093 (347.7)
CO stretch/a_1'	1056	1022	1216	1161	1147	1105 (0)

CCSD(T) levels. Moreover, at the coupled-cluster level, the basis set dependence is also unusually large. The curvature along the bend displacement changes from relatively stiff and positive (675 cm^{-1}, MP2) to much softer (CCSD/6-31G*) and, finally, negative values. Thus, D_{3h} minimum disappears at higher level of theory. Such strong variations are characteristic of vibronic interactions.

MCSCF calculations of Kaiser, Mebel, and co-workers[8,9] yield a very close set of frequencies for the C_{2v} structure and a vastly different results for D_{3h}. Moreover, they predict D_{3h} to be a stable minimum. They performed a series of MCSCF and MR-CI calculations using up to full-valence active space;[9] however, dynamical correlation was not included in calculating the optimized geometries and frequencies. Because vibronic interactions are very sensitive to the energy gap between the states, MCSCF results alone are not sufficient to conclude whether or not D_{3h} minimum exists—there are numerous examples of MCSCF predictions being reversed by inclusion of dynamical correlation.[17,28] Most importantly, when vibronic interactions are very strong, stationary points of adiabatic PES and harmonic vibrational frequencies do not provide qualitatively correct description of the molecular structure and properties. For example, in the NO_3 radical,[16] the explicit coupling between electronic and nuclear wave functions had to be taken into account to reproduce the experimental spectra. Even if D_{3h} minimum does not exist, the molecule can still behave as effectively D_{3h} if the PES is sufficiently flat.

Overall, our best estimate of C_{2v} frequencies agrees well with previously reported experimental values in CO_2 and in Ar matrices,[1,2,8] in agreement with earlier theoretical predictions.[5−8] Recently, Jamieson, Mebel, and Kaiser reported experimental detection of the D_{3h} isomer in solid CO_2.[10] Their assignment was based on the e′ CO stretch and the comparison between the computed and measured frequencies for several isotopomers. It should be noted that the changes in frequencies due to isotopic substitutions depend chiefly on the normal mode vector, which, in the case of small molecules, is largely determined by the molecular symmetry rather than the details of the PES. Our CCSD(T)/cc-pVTZ frequency of the measured mode agrees reasonably well with the experiment and the MCSCF value.

By symmetry, the e′ modes of the fully symmetric ground electronic state can only be coupled to the $^1E'$ excited states. There are two low-lying pairs of E′ singlets, as discussed in section 4.1. The JT behavior of these states decreases the gap and, therefore, enhances vibronic interactions. The states of E″ symmetry and the low-lying triplets do not interact with the ground state through eq 1; however, they can affect the stability of the RHF reference.

Vibronic interactions are closely related to HF instabilities and near-instabilities, as explained in ref 19. The stability analysis of the RHF wave function at D_{3h} revealed two RHF → UHF instabilities, e′ and e″, with the eigenvalues of −0.28 and −0.058, respectively. The more negative eigenvalue of the e′ instability is consistent with the E′ symmetry of the lowest triplet. No symmetry-breaking RHF → RHF instabilities were found; however, there are two near-instabilities within e″ and e′ blocks with 0.031 and 0.065 eigenvalues, respectively. Note that the lower eigenvalue is in e″ block, for example, consistent with the character of the lowest singlet. Because there are no e″ vibrational modes in CO_3, this near-instability does not directly affect quartic force constants.

Relative energies of the two structures are also very sensitive to the method employed, in agreement with previous studies. Table 4 summarizes total and relative energies of the isomers calculated by different methods. Due to the small HOMO−LUMO gap at D_{3h}, MP2 overestimates the corresponding correlation energy and places the D_{3h} isomer 49 kcal/mol below the C_{2v}. This is reversed at CCSD, which changes the ordering and yields energy separation of 23 kcal/mol in favor of C_{2v}. This value is reduced to 5.8 kcal/mol and 3.03 kcal/mol at the CCSD(T) and CCSDT levels, respectively. The relatively large effect of triple excitations is consistent with strong correlation at D_{3h}, and with considerable multiconfigurational character of the wave function, as reported by Mebel and co-workers.[9] The effects of the basis set beyond cc-pVTZ are less than 0.5

TABLE 4: Total Energies of the C_{2v} Isomer at the Corresponding Optimized Geometries and Relative Energy of D_{3h} Structure

method	$E_{tot}^{C_{2v}}$, hartree	$E_{tot}^{D_{3h}} - E_{tot}^{C_{2v}}$, kcal/mol
MRCI+Q(16,13)/6-311+G(3df)[a]		0.1
MP2/cc-pVTZ	−263.272926	−48.75
CCSD/cc-pVTZ	−263.260334	22.96
CCSD(T)/cc-pVTZ	−263.303902	5.81
CCSD(T)/cc-pVQZ[b]	−263.383049	6.07
CCSD(T)/aug-cc-pVTZ[b]	−263.323742	5.54
CCSDT/cc-pVTZ[b]	−263.360736	3.03
CCSDT/cc-pVQZ[c]	−263.439883	3.30
CCSDT/aug-cc-pVTZ[c]	−263.380576	2.76
CCSDT/aug-cc-pVQZ[c]	−263.459723	3.03

[a] ZPE-corrected, ref 8. [b] Calculated at the CCSD(T)/cc-pVTZ geometries. [c] Extrapolated, see text.

kcal/mol, and the extrapolated CCSDT/aug-cc-pVQZ value is the same as CCSDT/cc-pVTZ one.

To summarize, our results demonstrate that the vibronic interactions in CO_3 are very strong and have dramatic effect on the shape of the PES, which is rather flat along $D_{3h} \rightarrow C_{2v}$ displacements. Although the combined experimental and theoretical study of Jamieson, Mebel, and Kaiser[10] provides strong evidence of the D_{3h} isomer, the complete theoretical description of this molecule might require departure from harmonic description within adiabatic approximation.[16]

5. Conclusions

Ground-state equilibrium structures and frequencies of CO_3 are found to be affected by strong vibronic interactions with the low-lying excited states. We found that the existence of D_{3h} minimum strongly depends on the level of correlation treatment and basis set.

Low-lying excited singlet and triplet states are characterized at both geometries. The excited states ordering is quite unusual. For example, the relative ordering in the singlet and triplet manifolds is different, and the energy gaps between the singlet and triplet states of the same character are small. The JT character of the excited states at D_{3h} enhances the vibronic interactions.

Overall, our results suggest similarities with the NO_3 radical and that complete theoretical description of CO_3 may require explicit consideration of the couplings between electronic and nuclear degrees of freedom.[16] From the experimental point of view, the electronically excited states could provide a sensitive probe of the molecular structure, as the states ordering and character is very different at D_{3h} and C_{2v}.

Acknowledgment. Support from the National Science Foundation (CHE-0616271) and the WISE research fund (USC) is gratefully acknowledged. We thank Profs. Mitchio Okumura, Ralf Kaiser, and Alex Mebel for stimulating discussions and insightful comments. We also acknowledge the use of resources of the *iOpenShell* Center for Computational Studies of Electronic Structure and Spectroscopy of Open-Shell and Electronically Excited Species supported by the National Science Foundation through the CRIF:CRF CHE-0625419+0624602+0625237 grant.

References and Notes

(1) Moll, N. G.; Clutter, D. R.; Thompson, W. E. *J. Chem. Phys*. **1966**, *45*, 4469.
(2) Jacox, M. E.; Milligan, D. E. *J. Chem. Phys*. **1971**, *54*, 919.
(3) Pople, J. A.; Seeger, U.; seeger, R.; Schleyer, P. v. R. *J. Comput. Chem*. **1980**, *199*.
(4) Guchte, W. J. v. d.; Zwart, J. P.; Mulder, J. J. C. *J. Mol. Struct. (THEOCHEM)* **1986**, *152*, 213.
(5) Froese, R. D. J.; Goddard, J. D. *J. Phys. Chem*. **1993**, *97*, 7484.
(6) Averyanov, A. S.; Khait, Yu. G.; Puzannov, Yu. V. *J. Mol. Struct. (THEOCHEM)* **1999**, *94*, 459.
(7) Abreu, E. P.; Castro, M. A.; Costa, M. F.; Canuto, S. *J. Mol. Spectrosc*. **2000**, *202*, 281.
(8) Bennett, C. J.; Jamieson, C.; Mebel, A. M.; Kaiser, R. I. *Phys. Chem. Chem. Phys*. **2004**, *6*, 735.
(9) Mebel, A. M.; Hayashi, M.; Kislov, V. V.; Lin, S. H. *J. Phys. Chem. A* **2004**, *108*, 7983.
(10) Jamieson, C. S.; Mebel, A. M.; Kaiser, R. I. *Comput. Phys. Chem*. **2006**, *7*, 2508.
(11) Canutom, S.; Diercksen, G. H. F. *Chem. Phys*. **1987**, *120*, 375.
(12) Davidson, E. R.; Borden, W. T. *J. Phys. Chem*. **1983**, *87*, 4783.
(13) Crawford, T. D.; Stanton, J. F.; Allen, W. D.; Schaefer, H. F. J., III. *Chem. Phys*. **1997**, *107*, 10626.
(14) Stanton, J. F. *J. Chem. Phys*. **2001**, *115*, 10382.
(15) Russ, N. J.; Crawford, T. D.; Tschumper, G. S. *J. Chem. Phys*. **2005**, *120*, 7298.
(16) Stanton, J. F. *J. Chem. Phys*. **2007**, *126*, 134309.
(17) Vanovschi, V.; Krylov, A. I.; Wenthold, P. G. *Theor. Chim. Acta*, in press.
(18) Löwdin, P.-O. *Rev. Mod. Phys*. **1963**, *35*, 496.
(19) Crawford, T. D.; Kraka, E.; Stanton, J. F.; Cremer, D. *J. Chem. Phys*. **2001**, *114*, 10638.
(20) Koch, H.; Jørgen, Aa.; Jensen, H.; Jørgensen, P.; Helgaker, T. *J. Chem. Phys*. **1990**, *93*, 3345.
(21) Stanton, J. F.; Bartlett, R. J. *J. Chem. Phys*. **1993**, *98*, 7029.
(22) Levchenko, S. V.; Krylov, A. I. *J. Chem. Phys*. **2004**, *120*, 175.
(23) Hirata, S.; Nooijen, M.; Bartlett, R. J. *Chem. Phys. Lett*. **2000**, *326*, 255.
(24) Slipchenko, L. V.; Krylov, A. I. *J. Chem. Phys*. **2005**, *123*, 84107.
(25) Helgaker, T.; Jørgensen, P.; Olsen, J. *Molecular electronic structure theory*; John Wiley & Sons: New York, 2000.
(26) Shao, Y. et al. *Phys. Chem. Chem. Phys*. **2006**, *8*, 3172.
(27) Stanton, J. F.; Gauss, J.; Watts, J. D.; Lauderdale, W. J.; Bartlett, R. J. ACES II, 1993. The package also contains modified versions of the MOLECULE Gaussian integral program of J. Almlöf and P. R. Taylor, the ABACUS integral derivative program written by T. U. Helgaker, H. J. Aa. Jensen, P. Jørgensen and P. R. Taylor, and the PROPS property evaluation integral code of P. R. Taylor.
(28) Eisfeld, W.; Morokuma, K. *J. Chem. Phys*. **2000**, *113*, 5587.